Design and Performance Test of a Savonius Wind Turbine with Nok Putri Blades for Low Wind Speeds

Shanti Kumbarasari[1*], Ditta Pratama[2], Wahyu Arya Prayudana[1], Bernadine Gisyel Heing[1],

[1]Program Studi Teknik Mesin Industri, Politeknik Industri ATMI, Cikarang, 17520, Indonesia

[2] PT Tata Metal Lestari, Cikarang,17530, Indonesia

**Email Corresponding Author: shanti_kumbarasari@polinatmi.ac.id*

ABSTRAK

Pemanfaatan energi angin di kawasan industri berkecepatan angin rendah memerlukan turbin yang sederhana, murah, dan mudah difabrikasi. Penelitian ini merancang, membuat, dan menguji prototipe turbin angin sumbu vertikal tipe Savonius dengan bilah dari produk atap galvalume (nok putri) hasil produksi perusahaan manufaktur baja lapis di Cikarang. Metode meliputi pengukuran angin, pemilihan konsep dengan matriks morfologi dan skala Likert, estimasi teoretis, simulasi aliran dan struktur, uji lapangan tanpa beban, serta analisis biaya. Pengukuran selama 20 hari pada ketinggian 5,5 m memberikan kecepatan angin rata-rata 3,0 m/s dan maksimum 7,2 m/s. Konsep berbilah galvalume memperoleh skor 20 dibandingkan 16 untuk konsep berbilah NACA 4412. Simulasi struktur linear statis menghasilkan tegangan von Mises maksimum 0,113 MPa pada beban ekuivalen 110,5 N. Pada angin 1,2–3,7 m/s, prototipe berputar 16–24 rpm dengan tegangan terminal 6,7–9,6 V dan rasio kecepatan ujung 0,14–0,36; putaran ini hanya 5–8% dari putaran nominal generator 4 kW, yang mengindikasikan ketidaksepadanan rotor–generator. Daya dan koefisien daya tidak terukur karena pengujian dilakukan tanpa beban. Biaya investasi prototipe sebesar Rp13.958.332 lebih rendah 36,6% daripada turbin paket dan 27,0% daripada desain berbilah fiberglass. Nok putri memenuhi persyaratan awal sebagai bilah turbin angin Savonius dari sisi fabrikasi, struktur (simulasi), dan biaya, sedangkan kinerja aerodinamis dan listriknya masih perlu dibuktikan melalui uji berbeban.

Kata kunci: Galvalume; Kecepatan angin rendah; Savonius; Turbin angin sumbu vertikal

ABSTRACT

Harnessing wind energy in industrial areas with low wind speeds requires turbines that are simple, inexpensive, and easy to fabricate. This study designs, builds, and tests a vertical axis Savonius wind turbine prototype whose blades are made of a galvalume roofing product (nok putri, ridge cap) manufactured by a coated-steel company in Cikarang. The methods comprised wind measurement, concept selection with a morphological matrix and Likert-scale scoring, theoretical estimation, flow and structural simulations, a no-load field test, and a cost analysis. A 20-day measurement at 5.5 m height gave a mean wind speed of 3.0 m/s and a maximum of 7.2 m/s. The nok putri concept scored 20 versus 16 for the NACA 4412 blade concept. A linear static structural simulation produced a maximum von Mises stress of 0.113 MPa under an equivalent load of 110.5 N. At wind speeds of 1.2–3.7 m/s, the prototype rotated at 16–24 rpm with a terminal voltage of 6.7–9.6 V and a tip speed ratio of 0.14–0.36; this rotor speed was only 5–8% of the rated speed of the 4 kW generator, indicating a rotor–generator mismatch. Power and power coefficient were not measured because the test was conducted without load. The investment cost of the prototype, IDR 13,958,332, was 36.6% lower than a packaged turbine and 27.0% lower than a fiberglass-bladed design. Nok putri meets the initial requirements as a Savonius blade in terms of fabrication, structure (by simulation), and cost, whereas its aerodynamic and electrical performance remains to be demonstrated through loaded tests.

Keywords: Galvalume; Low wind speed; Ridge cap; Savonius; Vertical axis wind turbine

INTRODUCTION

Decarbonization of the industrial sector is a prerequisite for achieving Indonesia's *net zero emission* (NZE) target. Optimization scenarios show that emissions from energy-intensive industries could decrease from 466 MtCO2e to 56 MtCO2e by 2060, with new and renewable energy contributing about 37% of this mitigation [1]. The integration of renewable energy into the manufacturing industry still faces technical and economic challenges but also opens opportunities [2]. PT Tata Metal Lestari, a steel coated product manufacturing company in Cikarang, has utilized solar power plants (PLTS) on the *Continuous Galvanizing Line* (CGL) Cikarang and *Continuous Coating Line* (CCL) Sadang, and is now exploring wind as an additional renewable energy source.

Wind resources in Indonesia are relatively low, generally 2–5 m/s [3], so turbines capable of operating at low winds are relevant for development [4]. Vertical axis Savonius wind turbines driven by drag *are* suitable for this condition because their structure is simple, capable of rotating at low speeds, and receiving wind from all directions, although their efficiency is relatively low [5]. Recent research focuses on geometric parameters such as aspect ratio, number of levels, and torsional angle [6-8], *self-starting* characteristics [9], as well as flow augmentation techniques [10], [11]. Farozan et al. report power coefficients of 0.19–0.20 and the

lowest initial rotational speed of 2.5 m/s in low wind environments [8]. The effect of the number of blades was studied numerically [12] as well as experimentally [13], [14], and aerodynamic optimization based on CFD was widely performed [15]; under the same test conditions, two-blade rotors were reported to be more efficient than three-blade rotors because the addition of blades enlarged the inhibition surface [13].

From an electrical perspective, axial flux permanent magnet generators are widely used in small-scale turbines. At low winds, the aerodynamic power at *start-up* is small, so *cogging* torque must be pressed as low as possible to keep *cut-in* speed low [16]. The initial wind torque must also overcome *cogging* torque and mechanical friction [17], so *cogging torque* reduction in small wind generators continues to be studied [18]. Thus, the fit between rotor and generator is just as important as blade geometry.

These studies generally focus on optimizing blade geometry. The use of inexpensive or recycled materials for Savonius blades has been reported, for example used banner fabric [19], but with a focus on rotor geometry and layout. To the author's knowledge, the utilization of factory-available sheet metal products as Savonius turbine blades—thus reducing fabrication costs and time—is rarely studied alongside field testing at the factory site. The novelty of this research is: (i) the use of the company's galvalume princess cams as Savonius turbine blades; and (ii) the integrated design workflow which includes concept selection, flow and structure simulation, field testing, and cost analysis. In addition, test data were used to evaluate the suitability of rotor–generator at low winds as supporting findings. The objectives of this study are (1) characterizing the location wind (average and speed range), (2) selecting the concept and designing the prototype, (3) verifying the flow and strength of the structure through simulation, (4) testing the unloaded prototype and assessing its performance through rotation, terminal stress, and edge velocity ratio, and (5) comparing costs with other alternatives. The success criteria refer to company requirements: rotors spin at an average wind of about 3 m/s, the von Mises stress from the simulation is far below the material's yield strength, and the investment cost is lower than the alternatives compared.

RESEARCH METHOD

Object, Location, and Research Flow

The research object is the prototype of the Savonius wind power plant (PLTB) with a female blade. The research follows the flow in **Figure 1**. Wind surveys were conducted at PT TML Plant L3 Cikarang (2nd floor of the WTC building, height 5.5 m), material selection at Plant L10, fabrication at Plant L8, and prototype testing at Plant Sadang at a height of 3.5 m above the security post. Fabrication and assembly took place over 4 (4) days: *flange* and shaft welding, generator installation, blade and *chord installation*, and turbine installation on the support pole.



Figure 1 Research Flow

Wind Speed Measurement

Wind speed was measured using a Benetech digital anemometer type GM816A with an accuracy of 5%, with recording done every 1 minute for 20 days. For the first, second, and third days, they were divided into three sessions per day (morning, afternoon, and afternoon) lasting 30-45 minutes. Each session recorded average, minimum, and maximum values. Measurements were taken at a height of 5.5 m and not corrected to other heights. This data was used to determine the design conditions of 3 m/s (measured average value) and to establish three analysis cases, namely 3, 7, and 17 m/s.

Requirements and Concept Selection

Company requirements include the use of available products (nok putri and TASO light steel hollow), low cost, corrosion resistance for outdoor installation, ease of assembly and movement, and average wind rotation capability of about 3 m/s. The concept is arranged using a morphological matrix, which is a scheme to systematically combine partial solutions [20]. The function is divided into blades, blade–shaft connectors, and shafts; each has two alternatives, so there are $2 \times 2 \times 2 = 8$ combinations. Two integrated concepts were evaluated, namely Variant A (all alternatives A) and Variant B (all alternatives B, using products available according to company requirements); cross combinations were not evaluated. Variants were assessed on five aspects (performance, economy, ergonomics, durability, and features) on a Likert scale of 1–5 with

equal aspect weights, and the variant with the highest total score was selected; the effect of weights was reviewed through simple sensitivity analysis in the Results and Discussion section. Alternatives and considerations for each function are summarized in **Table 1**.

Table 1 Morphological Matrix and Key Considerations

Functions	Varian A	Varian B
Bilah (wind catcher)	NACA 4412 (lifting force). (+) higher rotation; (−) large initial energy, wide area	Nok putri C (resistive force). (+) rotates at low winds; (−) depends on flow pressure
Blade–shaft connector	Laser cutting *strip plate*. (+) easy to assemble; (−) requires *laser cutting process*	Hollow TASO 30 × 15 mm. (+) lightweight and strong; (−) easily dented during assembly
Rotational conductor	Solid cylinder. (+) strong; (−) heavy and expensive	Hollow pipe. (+) lightweight; (−) potentially curved

Prototype and System Specifications

The blade uses a galvalume (55% Al, 45% Zn) main shaft with standard width of 120 mm, curved radius of 95 mm, and length of 1,050 mm; the installed blade has an effective length of 850 mm and a total rotor height of 1,010 mm (**Table 2**). *The chord* uses TASO hollow 30 × 15 mm coated with galvalume, the shaft uses carbon steel pipe, and the joints use rivet nails and *tapping screws*. The generator is a three-phase axial flux permanent magnet generator (AFPM) of 4 kW at 300 rpm. The planned system consists of a turbine, generator, controller with converter, 12 V 120 Ah LiFePO4 battery, and DC–AC inverter; in this study, only turbines and generators were tested. Complete specifications, including rotor sweep area, are presented in **Table 2**.

Theoretical Estimation

The flow regime is determined by Reynolds numbers [21]

$$Re = \frac{\rho v L}{\mu} \quad (1)$$

with ρ air density (1.205 kg/m3), v wind speed, *rotor diameter* L (0.454 m), and *dynamic viscosity* μ of air (1.849×10−5 Pa·s at 20 °C). The vertical axis rotor sweep area and wind power are calculated by

$$A = D \times H \quad (2)$$

$$P_a = \frac{1}{2}\rho A V^3 \quad (3)$$

with D rotor diameter (0.454 m), H sweep height (effective blade length 0.85 m), and V wind speed. The theoretical upper limit of rotor power follows Betz's limit (16/27) [21]

$$P_B = \frac{16}{27} \cdot \frac{1}{2}\rho A V^3 \quad (4)$$

with a sweep area A equal to Equation (2). Betz's limit applies to all types of turbines as an absolute limit, whereas Savonius rotors based on drag force operate far below it, for example power coefficients 0.19–0.20 in lowwind studies [8]. All calculations use ρ = 1.205 kg/m3, D = 0.454 m, and H = 0.85 m.

Flow and Structure Simulation

Pressure distribution on two- and three-blade rotors at wind speeds of 3 m/s was compared with Cradle software, and the flow velocity pattern around the rotor was analyzed with SolidWorks (2022). The flow simulation setting is the turbine sweep area. This mesh area is up to a scale of 1-0.5 with laminar flow type in the steady simulation (stationary rotor). The number of blades (two or three) is not an alternative in the morphological matrix and is therefore reviewed separately through this flow simulation. Structural strength was analyzed using *the Autodesk Inventor Professional 2023 stress analysis module (static linear analysis) at equivalent wind loads of 19.5; 45.5; and 110.5 N for speeds of 3, 7, and 17 m/s (*Table 5). At a speed of 17 m/s, strong wind scenarios (Beaufort Scale 7, about 2.4 times the maximum measured speed) were used to test structural resistance, not site operating conditions. Input data from the *nexalume material structure model (galvalume)* thickness of 0.4 mm. The outputs evaluated were von Mises stress, *displacement*, and safety factor, as is common in element-to-turbine blade analysis [22].

Prototype Testing and Data Processing

Testing was conducted without load in the morning, afternoon, and afternoon for two days with 16 observations each. Wind speed was measured with a BENETECH anemometer type GM816A with a 5% accuracy tolerance. The turbine height was positioned at 1.5 meters from the ground surface, rotation N (rpm) measured using a tachometer type DT-2234C+ with specification accuracy of ± (0.05% + 1 digit) and terminal voltage *generator* U with AC mode equipped with a multimeter. The recording method (instantaneous or average) and synchronization of V, N, and U readings without loading with current is unreadable, so torque, current, and mechanical power are not measured and not reported as results. The only derivative calculated from the measured data is the *rotor* tip speed ratio

$$\lambda = \frac{\pi D N}{60 V} \quad (5)$$

with D = 0.454 m. The relationship between wind speed and rotation and stress was analyzed using least squared linear regression; regression coefficients were reported along with standard errors, 95% confidence intervals, and p-values. The regression results only applied to the tested speed range (1.2–3.7 m/s) and were not extrapolated.

Cost Analysis

Three options were compared: (A) Savonius wind power plant with female blades (this study);

(B) a one-set wind turbine package along with an electrical system from the online market; and (C) Savonius design with fiberglass blades. The cost scope for option A with a female blade is Rp 13,984,886 with a power output per day of Rp. 20.1802, and an output price per day of Rp. 1,090,180. option B is Rp 22,000,000 with a power output per day of Rp. 20.1802 and an output price per day of Rp. 1,090,180, and option C is Rp 19,113,397 with a power output per day of Rp. 25.2706 and an output price of Rp. 757,142. The theoretical daily energy is calculated from the Betz limit rotor power (Equation (4)) at 3 m/s over 24 hours; the energy of options B and C is derived from option A according to the sweep area ratio (+19% and +25%) and thus is not an independent measurement result. The cost indicator is expressed as

$$I_B = \frac{Harga}{24P_B} \quad (6)$$

in Rp per Wh/day. This indicator is only used for relative comparisons between options; because the energy of options B and C is derived from option A and is entirely based on theoretical limits, this indicator essentially compares cost per unit sweep area, not actual performance.

RESULTS AND DISCUSSION

Wind Characteristics Location

Measurements over 20 days produced an average wind speed of 3.0 m/s with a range of 0–7.2 m/s (**Table 3**). The average per session was relatively uniform, namely 2.8 m/s (morning), 3.1 m/s (afternoon), and 2.9 m/s (afternoon); these values were rounded to one decimal point so that the average of the three was not exactly the same as the overall average. The difference between sessions was only 0.3 m/s, while the data distribution (standard deviation and frequency distribution) had not been analyzed. A speed of 3 m/s is equivalent to 5.8 knots or Beaufort Scale 2 (gentle wind). At a rotor diameter of 0.454 m, the Reynolds number reaches 8.9×104 (Equation (1)). This condition is classified as low wind, consistent with the characteristics of Indonesian winds [3]. Data were measured at a height of 5.5 m at Plant L3 and were not converted to the height or prototype test location (3.5 m, Medium Plant), so they are used as a general overview and basis for determining design conditions, not as direct comparisons of test results. These conditions make the Savonius turbine based on candidate drag force plausible [5].

Table 3 Wind Speed Statistics

Parameter	Wind survey (5.5 m, Plant L3)	Prototype test (3.5 m, Medium Plant)
Duration	20 days	2 days (16 data)
Average (m/s)	3,0	2,56
Maximum (m/s)	7,2	3,7
Minimum (m/s)	0	1,2
Morning average (m/s)	2,8	–
Average day (m/s)	3,1	–
Average afternoon (m/s)	2,9	–

Concept Selection and Final Design

Variant A uses NACA 4412 profiled blades that utilize lift force, while variant B uses a putri ridge blade that resists flow (drag force) and is a product development for wind power plant applications (**Table 1**). **Table 4** shows that variant B excels with a score of 20 to 16, especially in performance (5 to 3), ergonomics (4 to 2), and economy (5 to 4), although lower in ease of assembly (2 to 3) because TASO hollows are prone to dents and hollow shafts have the potential to warp when assembled. These results align with the turbine's ability to rotate in low winds [5], [8]. A simple sensitivity analysis from **Table 4** shows that the score differences per aspect (B minus A) are +2, +1, +2, 0, and −1; if the feature aspect weight is increased to k times the weight of other aspects, the total difference becomes $5 - k$, so variant B remains superior for $k < 5$. Two limitations need to be noted. First, NACA 4412 is a lift type profile, so this comparison is between lift and inhibition type turbine concepts, not between Savonius blades; cross-combinations between alternatives are also not evaluated. Second, Likert scale assessments are subjective and should be read as a decision aid, not a performance measurement; actual performance is verified through simulations and field tests in the next section.

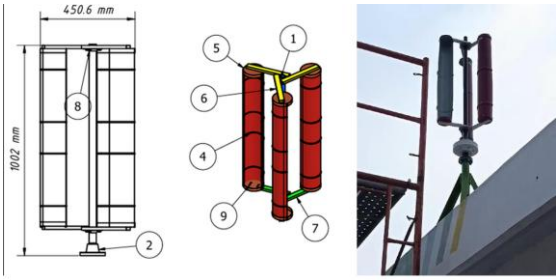
Table 4 Concept Variance Assessment (Likert Scale 1–5)

Aspects	Varian A	Varian B
Performance (spinning in wind ±3 m/s)	3	5
Economical (using *available parts*)	4	5
Ergonomic (location-appropriate, easy to move)	2	4
Durability (corrosion resistant, outdoors)	4	4
Features (ease of assembly)	3	2
Total score	**16**	**20**

Variant A: NACA 4412, strip plate, solid shaft. Variant B: nok putri, TASO 30 × 15, hollow pipe. 1 = not good, 5 = very good.

The final design consists of three closed princess ridge blades mounted parallel to the vertical shaft and connected to the shaft via *TASO hubs* at the top and bottom (**Figure 2a**). The fabricated prototype is mounted on a pole at Plant Sadang (**Figure 2b**), with specifications in **Table 2**. The height to rotor diameter ratio (H/D) is 0.85/0.454 ≈

1.9; The aspect ratio is one of the main geometric parameters of the Savonius rotor [6].



(a) **(b)**

Figure 2 (a) Working Drawings and CAD Rotor Model (1 Shaft, 2 *Flanges*, 4 Female Cams, 5 Female Cam Caps, 6–7 TASO Hubs); (b) Installed Prototype

Table 2 Wind Power Plant Prototype Specifications

Parameter	Specifications
Rotor type	Savonius (resistive force), vertical axis, three blades
Diameter rotor	454 mm
Blade length	850 mm
Total rotor height	1.010 mm
Massa rotor	6,5 kg
Bilah (Blade)	Nok putri galvalume (55% Al, 45% Zn), lebar 120 mm, R 95 mm, bertutup
Sweep area (D × H)	0,386 m^2 (0,454 m × 0,85 m)
Thickness of the Nok Putri plate	0.4 mm
Blade arc angle; overlap ratio	Sudut busur 120° : overlap ration 12,5%-20%
Chord/hub	Hollow TASO 30 × 15 mm (galvalume)
Shaft	Pipa baja karbon Ø34 mm/Ø28 mm
Binder	Paku rivet 58 buah, sekrup *tapping* 12 buah
Generator	AFPM 3 fasa, 4 kW, 300 rpm, 380 VAC, η > 80%, torsi awal < 0,2 N·m, 20 kg

Theoretical Estimation

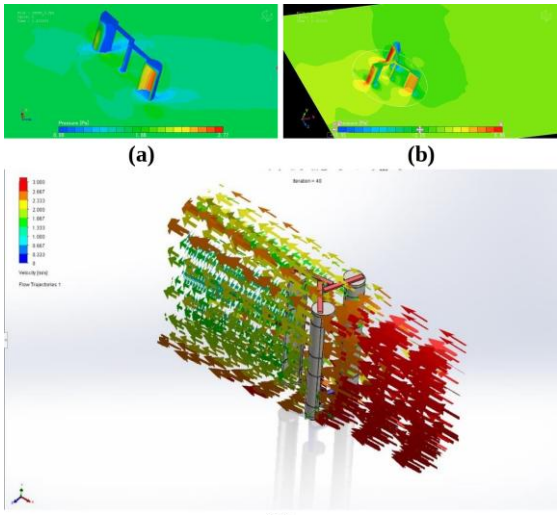
Table 5 summarizes theoretical estimates for the three speeds, calculated with the vertical axis rotor sweep area $A = D \times H = 0.454 \times 0.85 = 0.386$ m2 and $\rho = 1.205$ kg/m3. Wind power increases in cubic terms, from 6.28 W at 3 m/s to 1.142 W at 17 m/s, while Betz's rotor limit power is 3.72 W at 3 m/s. This value is an absolute theoretical upper limit, as the real Savonius power coefficient is far below the Betz limit (0.59); for example, 0.19–0.20 in low wind studies [8]. This cubic property means energy production depends heavily on wind speed, so wind fluctuations at the location (0–7.2 m/s) have a significant impact on daily energy. The last row **of Table 5** compares the equivalent load of the structural simulation with the static resistivity force 1/2ρV2A Cd over the same area, with the Cd inhibition coefficient assumed to be 1.2–2.0 (assumption, not measurement). The simulation loads are higher than the comparators at 3 and 7 m/s and fall within the comparison range at 17 m/s.

Table 5 Theoretical Estimation at Three Wind Speeds

Parameter	3 m/s	7 m/s	17 m/s
Skala Beaufort	2	4	7
Reynolds Number ($\times 10^4$)	8,88	20,7	50,3
P_a (W)	6,28	79,7	1.142
P_B (W)	3,72	47,3	677
Simulation load (N)	19,5	45,5	110,5
Comparative inhibition force, C_d 1,2–2,0 (N)	2,5–4,2	13,7–22,8	81–134

Flow and Structure Simulation

At 3 m/s, the pressure range on the two-blade rotor is 0–3.77 Pa, while on the three-blade rotor it is −10.95 to 6.86 Pa (**Figures 3a** and **3b**). The color scales of the two panels differ, so comparisons should be based on numerical ranges, not colors. A wider range on the three-blade rotor indicates a greater pressure difference between the upstream and downstream sides of the blades, in line with the observation that adding blades enlarges the resistance surface [13]. However, the pressure range is not torque or power coefficient: net torque depends on the force difference between the forward blade and the return blade, which is not calculated in this simulation. This result is therefore only indicative that the three-blade rotor receives greater inhibition loads at low winds and has not proven higher initial torque or efficiency; other experimental studies have reported higher peak efficiency of two-blade rotors [13]. In the 3 m/s flow simulation (**Figure 3c**), the speed after passing through the blade drops to 1.3–2 m/s, meaning the wind momentum is held back by the blade surface; this image was taken at the 40th iteration. Thus, the experimental verification of static torque of two- and three-blade rotors is further research.



(a) **(b)**

(c)

Figure 3 Simulation Results at 3 m/s: Pressure Distribution (a) Two Blades, (b) Three Blades; (c)

Flow Velocity Vector Around the Rotor; Color Scales (a) and (b) Different

The structural simulation results in **Table 6** show a maximum von Mises stress of 0.113 MPa and a maximum displacement of 4.47 mm in the heaviest case (17 m/s, 110.5 N), with stress concentrations around *hub* and blade joints (**Figure 4**). The safety factor is >15 in all cases, which exceeds the software output scale limit, so the actual value cannot be read from this simulation. Because the analysis is linear static, the stress is directly proportional to the load; even when the load of 17 m/s is raised to the upper limit of the comparative resistivity force (±134 N), the maximum stress is only ±0.14 MPa, far below the yield strength of coated steel, *galvalume* material containing 55% Al and 45% Zinc. Aluminum properties are lightweight, corrosion resistant, good conductivity of electricity and heat. The zinc element has characteristics of a bluish-white color, boiling point of 907°C, melting point 419.5°C, density of 7.14 g/cm3, with good thermal and electrical conductivity. The low stress indicates that structural strength does not appear to be a limiting factor in the analyzed velocity range. This analysis uses equivalent static loads and does not include dynamic loads, fatigue, thin plate bending, or resonance; Mesh convergence tests and experimental verification (e.g., strain or deflection tests) have not been conducted.

Table 6 Structural Simulation Results

V (m/s)	Load (N)	Von Mises (MPa)	Transfers (mm)	FK
3	19,5	0,017–0,040	0,955–1,032	>15
7	45,5	0,029–0,067	1,609–1,842	>15
17	110,5	0,071–0,113	3,908–4,472	>15

FK = security factor; >15 means exceeding the software output scale limit.

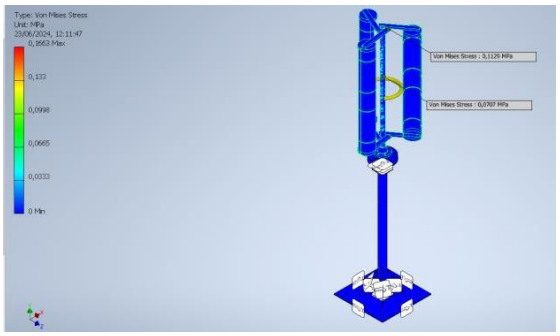


Figure 4 Von Mises Voltage Distribution at 17 m/s (Load 110.5 N)

Prototype Testing Results

The prototype was already rotating at the lowest observed wind speed (1.2 m/s); the initial rotational speed (*cut-in*) had not been determined because there were no observations at lower speeds. In the range of 1.2–3.7 m/s (average 2.56 m/s), rotor rotation 16–24 rpm (average 18.9 rpm) and terminal voltage 6.7–9.6 V (average 7.55 V) (**Table 7**). Linear regression yielded $N = 13.37 + 2.15V$ ($R2 = 0.48$; slope standard error 0.60; 95% confidence interval 0.87–3.44; $p = 0.003$) and $U = 5.35 + 0.86V$ ($R2 = 0.54$; standard error 0.21; 95% confidence interval 0.40–1.31; $p = 0.001$) (**Figures 5a** and **5b**). The positive trend is significant, but the moderate coefficient of determination indicates other factors, namely momentary wind fluctuations, roof turbulence, and limited data volume. This equation only applies in the range of 1.2–3.7 m/s. The intercept has no physical significance, because at $V = 0$ rotation and voltage should be zero; a large interception value reflects data limitations (16 points, five of which are at 2.8 m/s, so observations are not entirely independent) and measurement uncertainty. The end speed ratio calculated from the measured data is 0.14–0.36 (average 0.19) and decreases with rising wind speed (**Figure 5c**), meaning rotor rotation rises much more slowly than wind speed. Torque, current, and power are not measured and therefore not reported; power performance can only be determined through load tests with measurements of torque or current and voltage.

Table 7 Unloaded Prototype Test Results Data

V (m/s)	*N* (rpm)	*U* (V)	λ (calculated)
1,2	17	6,9	0,34
1,2	18	7,0	0,36
1,6	16	6,7	0,24
1,7	17	7,0	0,24
1,7	18	7,0	0,25
2,7	18	7,1	0,16
2,8	18	7,0	0,15
2,8	17	6,8	0,14
2,8	18	7,6	0,15
2,8	18	7,4	0,15
2,8	17	7,1	0,14
2,9	19	7,0	0,16
3,1	23	8,2	0,18
3,5	20	9,0	0,14
3,6	24	9,6	0,16
3,7	24	9,4	0,15

V, *N*, and *U* are the measurement results; λ is calculated from *V* and *N* using Equation (5). Data are sorted according to wind speed, not by observation time.

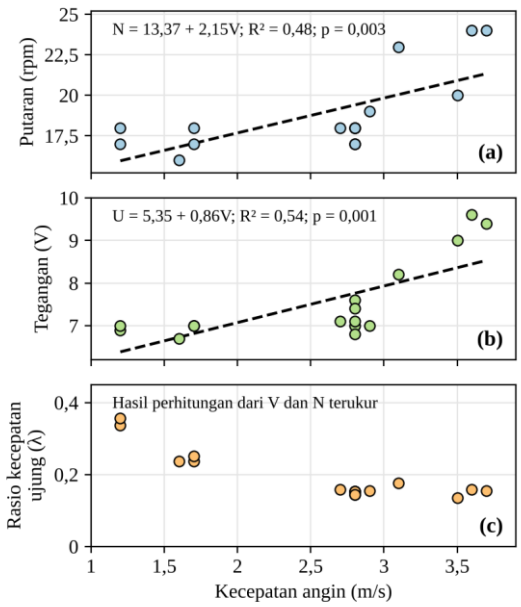


Figure 5 Relationship Between Wind Speed with (a) Rotation, (b) Voltage, and (c) Tip Speed Ratio

Measurable Performance Analysis and Suspected Causes of Low RPM

Measured performance showed the rotor spinning slowly compared to wind speed and nominal generator rotation: the tip speed ratio was only 0.14–0.36 (average 0.19) and the 16–24 rpm rotation was only 5.3–8.0% of the nominal rotation at 300 rpm. Because power and torque were not measured, the rotor power coefficient could not be stated and therefore was not compared to the power coefficient of 0.19–0.20 measured in the low wind study [8]. Three factors are thought to explain the low rotation but have not been tested separately.

First, the rotor rotates well below optimal conditions. The measured tip speed ratio (Equation (5)) is only 0.14–0.36, whereas the peak power of Savonius rotors is generally achieved at ratios less than 1 [13]; this study has not measured the free rotation of rotors without a generator, so the magnitude of the generator's influence is unknown. *Second*, the generator appears disproportionate to the rotor. Measured rotation is only 5.3–8.0% of nominal rotation. The terminal voltage is also lower than expected: when voltage is considered proportional to the rotation (380 V at 300 rpm, or 1.27 V/rpm), rotation of 16–24 rpm produces ±20–30 V, while measured is 6.7–9.6 V (0.36–0.45 V/rpm, or 28–36% of the nominal ratio). This difference cannot yet be explained from existing data and may be related to measurement configurations (phase or interphase voltage, rectifier) or AC current generator characteristics. The initial torque of the generator is listed as <0.2 N·m (upper limit of specifications); Because the rotor remains rotating at 1.2 m/s, aerodynamic torque at that speed is sufficient to overcome *cogging* torque and installed generator friction, but the actual torque value has not been measured. In low winds, *cogging* torque and friction are the main obstacles because aerodynamic torque is very low [16], [17]. *Third*, location conditions are not ideal: turbines are installed low (3.5 m) on the roof, causing uneven and turbulent flow, unlike uniform flow in simulations. Testing is also loadless and only two days.

This discrepancy can be roughly quantified. The nominal power of the generator (4 kW) is about 1,100 times the rotor power limit of Betz at 3 m/s (3.72 W), and about 6 times that power at 17 m/s (677 W); because the actual rotor power is less than the Betz limit, the actual ratio is greater. Nominal speed at 300 rpm is almost 16 times the average measured speed (18.9 rpm). When the rotor is operated at a design tip speed ratio of 0.75, the angular speed at 3 m/s is 0.75 × 3/0.227 ≈ 9.9 rad/s or ±95 rpm (0.227 m is the rotor radius), so a rotation booster transmission of about 3:1 is required to reach 300 rpm; Under measured conditions (tip speed ratio 0.19), the requirement approaches 16:1. These figures indicate that generators need to be selected based on power and rotor rotation, not the other way around.

Thus, the most consistent assumption with the data is that the low rotation and voltage are mainly related to the selection of a 4 kW generator with a nominal rotation of 300 rpm for a rotor diameter of 0.454 m, not due to the limitation of the Putri nok as a blade. This assumption has not been tested because there is no control test (free rotation without a generator or other blade comparators under the same conditions), so the aerodynamic feasibility of the Putri Nose Blade cannot yet be determined. From the initial requirements side, the Putri Nose allows the rotor to rotate at winds of 1.2–3.7 m/s, uses available products, and is safe in structural simulations. Realistic improvements are low-turn, low-power AFPM generators with *low cogging* torque [18], booster thrust transmissions (e.g., *pulley-belts*), installation at higher locations, and load testing to measure actual current and power. From an NZE policy perspective, a single rotor of this scale has not made a real contribution to the plant's power supply; its main value is demonstrating that industrial products can be assembled into Savonius rotors rotating at low winds and identifying critical parameters for further development.

Cost Analysis

The cost of the female nok prototype (Rp13,958,332) is 36.6% lower than the package turbine and 27.0% lower than the fiberglass blade design (**Table 8**). Per theoretical daily energy unit, option A is 24.6% and 8.6% cheaper, respectively. Because the energy of options B and C is derived from option A through the sweep area ratio, the difference per unit energy essentially reflects the price per unit sweep area, not the performance

difference. This indicator also assumes a constant wind of 3 m/s for 24 hours and Betz limit power, so it is only feasible for relative comparison; the actual energy is much smaller because the measured tip velocity ratio is only 0.14–0.36, and the value can only be confirmed through load testing. In a 12 kW turbine case study in Malaysia, about 75% of total wind energy costs come from initial investments [23]; the scale and context differ, but show that absolute economic benefits can only be assessed if output power is measured and increased through generator improvements.

Table 8 Cost Comparison of Three Wind Power Plant Options

Opsi	Cost (Rp)	Energy (Wh/day)	I_B (Rp per Wh/day)
A. Savonius bilah nok putri (Savonius blade)	13.958.332	89,28	156.340
B. 1 set turbine package + electrical system	22.000.000	106,14	207.277
C. Savonius bilah (Savonius blade) fiberglass	19.133.397	111,80	171.137

The energy of options B and C is derived from option A according to the sweep area ratio; all energy values are based on the Betz limit at 3 m/s over 24 hours (theoretical value, not measurable).

Occupational Care and Safety

As a complement to the design outside the research objectives and without quantitative data, routine maintenance includes cleaning the blades, shafts, *chords*, and generators from dust, oil, and leaves; inspecting the blades for corrosion, bending, and deformation; checking the *tightness of chord* screws; as well as crack inspection of *base plate* and pole welds. Occupational safety follows a risk control hierarchy: elimination (turbines installed away from people, trees, buildings, and electrical cables), substitution (*stainless steel flanges* replaced with S45C, generator frame locks replaced with keyway bolts for easier disassembly, and table-shaped frames replaced *base plates* with pipes), modifications (fiberglass blades replaced with female cams and H rotors replaced with simpler Savonius), as well as level 1 personal protective equipment (goggles, helmets, *safety shoes*, and *wearpacks*) that must be used, with reporting of every incident through forms.

CONCLUSION

This study designed, manufactured, and tested a prototype of a Savonius turbine with a female ridge blade with the following findings. First, the location wind was relatively low (average 3.0 m/s; maximum 7.2 m/s), so a Savonius turbine based on drag force was appropriately considered. Second, the morphology matrix and Likert assessment placed the ridge blade concept above the NACA 4412 concept (score 20 to 16), and the three-blade design was successfully fabricated with a rotor mass of 6.5 kg; this assessment is subjective and only compares the two integrated concepts. Third, static linear structure simulations show a maximum von Mises stress of 0.113 MPa at an equivalent load up to 110.5 N, so the structural strength does not appear to be limited within the analyzed range. Fourth, the no-load test at winds of 1.2–3.7 m/s produced a rotation of 16–24 rpm, terminal voltage of 6.7–9.6 V, and an end velocity ratio of 0.14–0.36; rotor rotation was only 5–8% of the nominal rotation of a 4 kW generator (300 rpm), indicating a rotor–generator mismatch, but this assumption has not been tested with control tests, and the rotor's power and power coefficient have not been measured. Fifth, the prototype investment cost is 36.6% lower than the package turbine and 27.0% lower than the fiberglass blade design, while the ratio per unit of energy is theoretical. Thus, the feasibility of the female nok as a new Savonius turbine blade is demonstrated in terms of concept, fabrication, structure (simulation), and investment cost; Aerodynamic feasibility and electrical power require further research including load testing with torque measurement, free rotation tests without generators, rotating generators with low initial torque or booster transmissions, as well as installation at higher locations.

ACKNOWLEDGMENTS

The author expresses gratitude to PT Tatalogam Lestari, PT Tata Metal Lestari for material support, fabrication facilities, and testing locations, as well as to ATMI Industrial Polytechnic for academic support.

REFERENCES

[1] Utama PA, Gielbert MA, Revitasari R, Reyseliani N, Purwanto WW. Assessing decarbonization pathways for energy-intensive industries in Indonesia using TIMES optimization model. Energy and Climate Change 2025; 6: 100202. https://doi.org/10.1016/j.egycc.2025.100202

[2] Usman FO, Ani EC, Ebirim W, Montero DJP, Olu-lawal KA, Ninduwezuor-Ehiobu N. Integrating renewable energy solutions in the manufacturing industry: challenges and opportunities: a review. Engineering Science & Technology Journal 2024; 5(3): 674-703.

[3] Herlambang YD, Supriyo, Prasetiyo B, Mulud TH. Unjuk kerja turbin Savonius menggunakan generator sinkron magnet permanen pada variasi pembebanan dan kecepatan angin yang berbeda. Jurnal Rekayasa Mesin 2021; 16(2): 272-278.

[4] Langer J, Simanjuntak S, Pfenninger S, Laguna AJ, Lavidas G, Polinder H, et al. How offshore wind could become economically

attractive in low-resource regions like Indonesia. iScience 2022; 25: 104945. https://doi.org/10.1016/j.isci.2022.104945

[5] Chitura AG, Mukumba P, Lethole N. Enhancing the performance of Savonius wind turbines: a review of advances using multiple parameters. Energies 2024; 17(15): 3708. https://doi.org/10.3390/en17153708

[6] Cuevas-Carvajal N, Cortes-Ramirez J, Norato JA, Hernandez C, Montoya-Vallejo M. Effect of geometrical parameters on the performance of conventional Savonius VAWT: a review. Renewable and Sustainable Energy Reviews 2022; 161: 112314. https://doi.org/10.1016/j.rser.2022.112314

[7] Prabowoputra DM, Prabowo AR. Effect of geometry modification on turbine performance: mini-review of Savonius rotor. International Journal of Mechanical Engineering and Robotics Research 2022; 11(10): 777-783.

[8] Farozan I, Soelaiman TAF, Soetikno P, Indartono YS. The effect of rotor aspect ratio, stages, and twist angle on Savonius wind turbine performance in low wind speeds environment. Results in Engineering 2025; 25: 104041.

[9] Shamsuddin M, Kamaruddin NM. Experimental study on the characterization of the self-starting capability of a single and double-stage Savonius turbine. Results in Engineering 2023; 17: 100854.

[10] Karmakar SD, Chattopadhyay H. A review of augmentation methods to enhance the performance of vertical axis wind turbine. Sustainable Energy Technologies and Assessments 2022; 53: 102469.

[11] Altan BD, Gungor A. Examination of the effect of triangular plate on the performances of reverse rotating dual Savonius wind turbines. Processes 2022; 10(11): 2278. https://doi.org/10.3390/pr10112278

[12] Halmy MSM, Didane DH, Afolabi LO, Al-Alimi S. Computational fluid dynamics (CFD) study on the effect of the number of blades on the performance of double-stage Savonius rotor. CFD Letters 2021; 13(4): 1-10. https://doi.org/10.37934/cfdl.13.4.110

[13] Ali MH. Experimental comparison study for Savonius wind turbine of two & three blades at low wind speed. International Journal of Modern Engineering Research 2013; 3(5): 2978-2986.

[14] Wenehenubun F, Saputra A, Sutanto H. An experimental study on the performance of Savonius wind turbines related with the number of blades. Energy Procedia 2015; 68: 297-304.

[15] Farajyar S, Ghafoorian F, Mehrpooya M, Asadbeigi M. CFD investigation and optimization on the aerodynamic performance of a Savonius vertical axis wind turbine. Sustainability 2023; 15(6): 5318. https://doi.org/10.3390/su15065318

[16] Dehshiri M, Ketabi A. A coreless axial flux-switching generator for micro-wind turbine application. Energy Science & Engineering 2022; 10(12): 4804-4813. https://doi.org/10.1002/ese3.1309

[17] Kim D-H, Pyo H-J, Kim W-H, Lee J, Lee K-D. Design of spoke-type permanent magnet synchronous generator for low capacity wind turbine considering magnetization and cogging torques. Machines 2023; 11(2): 301. https://doi.org/10.3390/machines11020301

[18] Kang J, Lee J, Ham S, Chun Y, Kim H. A study on new straight shape design to reduce cogging torque of small wind power generator. Machines 2024; 12(6): 412. https://doi.org/10.3390/machines12060412

[19] Im H, Kim B. Power performance analysis based on Savonius wind turbine blade design and layout optimization through rotor wake flow analysis. Energies 2022; 15(24): 9500. https://doi.org/10.3390/en15249500

[20] Pahl G, Beitz W, Feldhusen J, Grote K-H. Engineering design: a systematic approach. 3rd ed. London: Springer; 2007.

[21] Manwell JF, McGowan JG, Rogers AL. Wind energy explained: theory, design and application. 2nd ed. Chichester: Wiley; 2009.

[22] Hoque KN, Chowdhury SA, Haque SA. Structural analysis of wind turbine blade by using finite element method. Journal of Maritime Research 2023; 20(3): 224-239.

[23] Azmi A, Sebayang AH, Harjon A. Life cycle cost analysis and payback period of 12-kW wind turbine for a remote telecommunications base station in Malaysia. Aceh International Journal of Science and Technology 2023; 12(2): 304-316. https://doi.org/10.13170/aijst.12.2.33010

[24] IEC 61400-12-1:2022. Wind energy generation systems – Part 12-1: Power performance measurements of electricity producing wind turbines. Geneva: International Electrotechnical Commission; 2022.